REPORT DOCUMENTATION PAGE

Form Approved OMB NO. 0704-0188

1. REPORT DATE (DD-MM-YYYY)	2. REPORT TYPE	3. DATES COVERED (From - To)
09-01-2014	Final Report	5-Jun-2009 - 4-Jun-2013

4. TITLE AND SUBTITLE
Photo-healable Metallosupramolecular Polymers

5a. CONTRACT NUMBER
W911NF-09-1-0288

5b. GRANT NUMBER

5c. PROGRAM ELEMENT NUMBER
611102

6. AUTHORS
Stuart Rowan, Christoph Weder

5d. PROJECT NUMBER

5e. TASK NUMBER

5f. WORK UNIT NUMBER

7. PERFORMING ORGANIZATION NAMES AND ADDRESSES
Case Western Reserve University
10900 Euclid Avenue
White Building
Cleveland, OH 44106 -7015

8. PERFORMING ORGANIZATION REPORT NUMBER

9. SPONSORING/MONITORING AGENCY NAME(S) AND ADDRESS (ES)
U.S. Army Research Office
P.O. Box 12211
Research Triangle Park, NC 27709-2211

10. SPONSOR/MONITOR'S ACRONYM(S)
ARO

11. SPONSOR/MONITOR'S REPORT NUMBER(S)
56009-CH.15

12. DISTRIBUTION AVAILIBILITY STATEMENT
Approved for Public Release; Distribution Unlimited

13. SUPPLEMENTARY NOTES
The views, opinions and/or findings contained in this report are those of the author(s) and should not contrued as an official Department of the Army position, policy or decision, unless so designated by other documentation.

14. ABSTRACT
This research project is focused on the development and investigation of a class of metallo-supramolecular polymers, which exhibit photo-induced healing capabilities. In this final report we outline the use of cellulose nanocrystals embedded within the metallosupramolecular polymer to access more mechanically robust photohealable films. We also outline initial investigations into a new class of Fe(II)-based metallosupramolecular polymers which can be healed at lower light intensities allowing access to a wider variety of photo-healable coatings.

15. SUBJECT TERMS
healable polymers, metal-ligand coordination, light, nanocomposites

16. SECURITY CLASSIFICATION OF:			17. LIMITATION OF ABSTRACT	15. NUMBER OF PAGES	19a. NAME OF RESPONSIBLE PERSON
a. REPORT	b. ABSTRACT	c. THIS PAGE			Stuart Rowan
UU	UU	UU	UU		19b. TELEPHONE NUMBER 216-368-4242

Report Title

Photo-healable Metallosupramolecular Polymers

ABSTRACT

This research project is focused on the development and investigation of a class of metallo-supramolecular polymers, which exhibit photo-induced healing capabilities. In this final report we outline the use of cellulose nanocrystals embedded within the metallosupramolecular polymer to access more mechanically robust photohealable films. We also outline initial investigations into a new class of Fe(II)-based metallosupramolecular polymers which can be healed at lower light intensities allowing access to a wider variety of photo-healable coatings.

Enter List of papers submitted or published that acknowledge ARO support from the start of the project to the date of this printing. List the papers, including journal references, in the following categories:

(a) Papers published in peer-reviewed journals (N/A for none)

Received		Paper
01/08/2014	12.00	Stuart J. Rowan, Christoph Weder, Gina L. Fiore. Optically healable polymers, Chemical Society Reviews, (11 2013): 0. doi: 10.1039/c3cs35471g
01/26/2012	7.00	Justin R. Kumpfer, Jeong J. Wie, John P. Swanson, Frederick L. Beyer, Michael E. Mackay, Stuart J. Rowan. Influence of Metal Ion and Polymer Core on the Melt Rheology of Metallosupramolecular Films, Macromolecules, (01 2012): 0. doi: 10.1021/ma201659d
01/26/2012	6.00	Mark Burnworth, Stuart J. Rowan, Christoph Weder. Structure–Property Relationships in Metallosupramolecular Poly(p-xylylene)s, Macromolecules, (01 2012): 0. doi: 10.1021/ma202312x
08/04/2011	3.00	Rudy J. Wojtecki, Michael A. Meador, Stuart J. Rowan. Using the dynamic bond to access macroscopically responsive structurally dynamic polymers, Nature Materials, (01 2011): 14. doi: 10.1038/nmat2891
08/04/2011	4.00	Mark Burnworth, Liming Tang, Justin R. Kumpfer, Andrew J. Duncan, Frederick L. Beyer, Gina L. Fiore, Stuart J. Rowan, Christoph Weder. Optically healable supramolecular polymers, Nature, (04 2011): 334. doi: 10.1038/nature09963
08/30/2012	9.00	Gina L. Fiore, Stuart J. Rowan, Christoph Weder . Light-Activated Healing of MetallosupramolecularPolymers, CHIMIA, (09 2011): 745. doi:
TOTAL:		**6**

Number of Papers published in peer-reviewed journals:

(b) Papers published in non-peer-reviewed journals (N/A for none)

Received	Paper

TOTAL:

Number of Papers published in non peer-reviewed journals:

(c) Presentations

Rowan:

July 2013 Department of Chemistry, Tsinghua University, Beijing, China
Invited Lecture: Using Dynamic Chemistry to Access Stimuli-Responsive Materials

July 2013 Lu Jiaxi Lectureship, Department of Chemistry, Xiamen University, Xiamen, China
Award Lecture: Using Dynamic Chemistry to Access Stimuli-Responsive Materials

June 2013 Department of Chemistry, Nanjing University, Nanjing, China
Invited Lecture: Using Dynamic Chemistry to Access Stimuli-Responsive Materials

June 2013 Department of Chemistry, Nanjing University, Nanjing, China
Invited Lecture: Using Dynamic Chemistry to Access Stimuli-Responsive Materials

June 2013 Department of Polymer Science, Fudan University, Shanghai, China
Invited Lecture: Using Dynamic Chemistry to Access Stimuli-Responsive Materials

June 2013 Gordon Research Conference, Mt Holyoke, Massachusetts
Invited Lecture: Structurally Dynamic Polymers as a Route to Adaptive Materials

Apr. 2013 University of Southern Mississippi, Bayer Distinguished Lectureship
Award Lecture: Structurally Dynamic Polymers: From Optically-Healable Materials to Mechanically-Adaptive Films

Apr. 2013 ANTEC, Cincinnati, Ohio
Invited Lecture: Structurally Dynamic Polymers as a Route to Stimuli-Responsive Materials

Apr. 2013 ACS PMSE/Chinese Chemical Society meeting, CWRU, Ohio
Invited Lecture: Supramolecular Approaches to Stimuli-Responsive Materials

Mar 2013 Department of Chemistry, Columbia University, New York
Invited Lecture: Structurally Dynamic Polymers: From Optically-healable Materials to Mechanically-adaptive Films.

Feb 2013 Material Science, Texas A&M, College Station, Texas
Invited Lecture: Structurally Dynamic Polymers: From Optically-healable Materials to Mechanically-adaptive Films.

Jan 2013Department of Chemistry, University of Maryland, Maryland
Invited Lecture: Supramolecular Approaches to Stimuli-Responsive Materials.

Jan 2013Department of Chemistry, Florida State University, Tallahassee, Fl
Invited Lecture: Structurally Dynamic Polymers as a Route to Stimuli-Responsive Materials.

Dec 2012 US-Japan Polymer Chemistry Symposium, Santa Barbara, US
Invited Lecture: Structurally Dynamic Polymers as a Route to Stimuli-Responsive Materials.

Nov 2012 PPG, Pittsburgh, Pa
Invited Lecture: Structurally Dynamic Polymers: From Optically-healable Materials to Mechanically-adaptive Films

Oct. 2012 8th International Symposium on Stimuli-responsive Materials, Santa Rosa, CA
Invited Lecture: Structurally Dynamic Polymers as a Route to Stimuli-Responsive Materials.

Sept. 2012 Department of Chemistry, University of Leeds, UK
Invited Lecture: Supramolecular Approaches to Stimuli-responsive Polymers

Sept. 2012 21st International Conference on Physical Organic Chemistry, Durham, UK
Invited Lecture: Stimuli-responsive supramolecular materials.

Weder:

Aug 2013 2nd Precision Polymer Materials (P2M) Conference, Ghent, Belgium
Invited lecture: Stimuli-Responsive Supramolecular Polymers

June 2013 University of Freiburg, Freiburg, Germany
Invited IRTG Seminar: Exploiting Non-Covalent Interactions for the Design of Stimuli-Responsive Polymers

May 2013 Chulalongkorn University,; Bangkok, Thailand
Invited lecture: Healing Polymers with Light and other Stimuli

May 2013 Jiao Tong University, Shanghai, China
Invited lecture: Stimuli-Responsive Polymers based on Noncovalent Interactions

May 2013 48th Bürgenstock Conference, Brunnen, Switzerland
Invited lecture: Stimuli-Responsive Polymers based on Noncovalent Interactions

April 2013 ACS 2013 Spring Meeting, April 8, 2013; New Orleans, LA, USA
Invited lecture: From Light-Polarizing Films and Semiconducting Polymer Networks to Mechano-Healable Polymers

Jan 2013University of Bayreuth, Bayreuth, Germany
Invited GDCh Seminar: From Light-Polarizing Films and Semiconducting Polymer Networks to Mechano-Healable Polymers

Dec 2012 International Polymer Congress 2012, Kobe, Japan
Invited Lecture: Stimuli-Responsive Polymers based on Noncovalent Interactions

Dec 2012 Department of Chemistry, Waseda University, Tokyo, Japan
Invited Lecture: Exploiting Supramolecular Interactions for the Design of Functional Polymers

Nov 2012 DPI Annual Meeting, Zeist, The Netherlands
Invited Lecture: Stimuli-Responsive Polymers Based on Non-Covalent Interactions

Fiore:

Sep 2013 International Soft Matter Conference 2013, Rome, Italy

Lecture: Mechanochemistry in Materials with Metal-Ligand Supramolecular Crosslinks
Sep 2013 Bioorganische Chemie 2013, Münster, Germany
Lecture: Mechanochemistry in Metallosupramolecular Materials
July 2013 Frimat Day 2013, Marly, Switzerland
Lecture: Mechanochemistry with Metallosupramolecular Materials
June 2013 PolyColl 2013, Basel, Switzerland
Lecture: Mechanochemistry of Metallosupramolecular Polymers
June 2013 EPF 2013, Pisa, Italy
Lecture: Mechanochemistry of Supramolecular Materials Containing Metal-Ligand Crosslinks and Built-In Optical Sensors
May 2013 Gordon Research Conference,; Les Diablerets, Switzerland
Invited Lecture: "Mechanochemistry in Lanthanide-Containing Metallosupramolecular Materials"
May 2013 SoftComp Annual Meeting, Rimini, Italy
Lecture: Metallosupramolecular Polymers: From Self-Healing Materials to Reversible Adhesives and More
April 2013 ACS National Meeting, New Orleans, Louisiana USA
Lecture Optically-Triggered Healing and Adhesive Properties of Metallosupramolecular Materials"

Number of Presentations: 36.00

Non Peer-Reviewed Conference Proceeding publications (other than abstracts):

Received	Paper
08/26/2012	10.00 Gina L. Fiore, Mark Burnworth, Liming Tang, Stuart J. Rowan, Christoph Weder. Reinforcement of Self-Healing Polymer Films with Cellulose Nanowhiskers, ACS PMSE Polym. Preprints. 27-MAR-11, . : ,
TOTAL:	**1**

Number of Non Peer-Reviewed Conference Proceeding publications (other than abstracts):

Peer-Reviewed Conference Proceeding publications (other than abstracts):

Received	Paper
TOTAL:	

Number of Peer-Reviewed Conference Proceeding publications (other than abstracts):

(d) Manuscripts

Received		Paper
01/08/2014	11.00	Souleymane Coulibaly, Anita Roulin, Sandor Balog,, Mahesh V. Biyani,, E. Johan Foster,, Stuart J. Rowan,, Gina L. Fiore,, Christoph Weder. Reinforcement of Optically Healable Supramolecular Polymers with Cellulose Nanocrystals, Macromolecules (10 2013)
01/09/2014	13.00	Souleymane Coulibaly, Diederik W. R. Balkenende, Sandor Balog, Yoan C. Simon, Gina L. Fiore, Christoph Weder. Mechanochemistry with Metallosupramolecular Polymers, Nature Chemistry (submitted) (12 2013)
01/09/2014	14.00	Christian Heinzmann, Souleymane Coulibaly, Anita Roulin, Gina L. Fiore, Christoph Weder. Light-Induced Bonding and Debonding with Supramolecular Adhesives, ACS Applied Materials and Interfaces (11 2013)
08/04/2011	5.00	Justin R. Kumpfer, Jeong J. Wie, John P. Swanson, Frederick L. Beyer, Michael E. Mackay, Stuart J. Rowan. Influence of Metal Ion and Polymer Core on the Melt Rheology of Metallo-Supramolecular Films, Macromolecules (08 2011)
09/22/2010	2.00	Mark Burnworth, Liming Tang, Justin R. Kumpfer, Andrew J. Duncan, Frederick L. Beyer, Stuart J. Rowan, Christoph Weder. Optically Healable Supramolecular Polymers, Nature (09 2010)
09/22/2010	1.00	Rudy J. Wojtecki, Michael A. Meador, Stuart J. Rowan. Using the Dynamic Bond to Access Macroscopically-Responsive Structurally-Dynamic Polymers, (09 2010)
TOTAL:	**6**	

Number of Manuscripts:

Books

Received	Paper
TOTAL:	

Patents Submitted

Patents Awarded

Awards

Stuart J. Rowan:
2013 Lu Jiaxi Lectureship, Xiamen University, China
2013 Bayer Lectureship, University of Southern Mississippi, USA

Graduate Students

NAME	PERCENT_SUPPORTED	Discipline
Adriane Miller	1.00	
Dirk Balkenende	1.00	
Souleymane Coulibaly	1.00	
FTE Equivalent:	**3.00**	
Total Number:	**3**	

Names of Post Doctorates

NAME	PERCENT_SUPPORTED
FTE Equivalent:	
Total Number:	

Names of Faculty Supported

NAME	PERCENT_SUPPORTED	National Academy Member
Stuart J Rowan	0.02	
Christoph Weder	0.02	
FTE Equivalent:	**0.04**	
Total Number:	**2**	

Names of Under Graduate students supported

NAME	PERCENT_SUPPORTED	Discipline
Colleen Kennedy	0.00	Chemical Engineering
FTE Equivalent:	**0.00**	
Total Number:	**1**	

Student Metrics

This section only applies to graduating undergraduates supported by this agreement in this reporting period

The number of undergraduates funded by this agreement who graduated during this period: 0.00

The number of undergraduates funded by this agreement who graduated during this period with a degree in science, mathematics, engineering, or technology fields:..... 0.00

The number of undergraduates funded by your agreement who graduated during this period and will continue to pursue a graduate or Ph.D. degree in science, mathematics, engineering, or technology fields:..... 0.00

Number of graduating undergraduates who achieved a 3.5 GPA to 4.0 (4.0 max scale):..... 0.00

Number of graduating undergraduates funded by a DoD funded Center of Excellence grant for Education, Research and Engineering:..... 0.00

The number of undergraduates funded by your agreement who graduated during this period and intend to work for the Department of Defense 0.00

The number of undergraduates funded by your agreement who graduated during this period and will receive scholarships or fellowships for further studies in science, mathematics, engineering or technology fields: 0.00

Names of Personnel receiving masters degrees

NAME

Total Number:

Names of personnel receiving PHDs

NAME

Total Number:

Names of other research staff

NAME PERCENT_SUPPORTED

FTE Equivalent:
Total Number:

Sub Contractors (DD882)

Inventions (DD882)

Scientific Progress

See Attachment

Technology Transfer

Photo-Healable Supramolecular Polymers

Proposal No: 56009CH

Agreement No: W911NF0910288

PIs Stuart Rowan and Christoph Weder

Department of Macromolecular Science and Engineering

Case Western Reserve University

2100 Adelbert Road

Cleveland, OH 44106-7202

and

Adolphe Merkle Institute and Fribourg Center for Nanomaterials,

University of Fribourg, CH-1700, Fribourg, Switzerland.

Final Report Aug 2013

Scientific Progress and Accomplishments

Table of Contents

1.1 Photo-healable Nanocomposites

Introduction

Mechanical malfunctions of polymeric materials are often the result of crack formation and propagation until the material eventually fails.[1] To address this problem and to extend the lifetime and functionality of polymer-based products, researchers have recently developed several approaches to create self-healing or healable polymers, which have the ability to repair themselves autonomously (self-healing materials) or can be healed upon exposure to an external stimulus such as heat, light, pressure, or mechanical stress (healable materials). One attractive approach to create such healable materials is the use of supramolecular polymers.[2] These materials are assembled on the basis of non-covalent binding motifs and can, when healing action is desired, be temporarily disassembled upon exposure to an external stimulus. Many of the healable supramolecular polymers studied to date are physically or covalently cross-linked networks with a low glass transition temperature and therefore display moderate strength and stiffness under ambient conditions.

We[3] and many others have shown previously that low-modulus polymers can be efficiently reinforced upon introduction of rigid, high-aspect-ratio cellulose nanocrystals (CNCs) isolated by hydrolysis of natural cellulose.[4] Recently, we used this concept to reinforce supramolecular healable polymers based on π–π interactions with unmodified CNCs isolated from the mantles of tunicates.[5] Some of us extended this approach to create light-healable nanocomposites based on a telechelic poly(ethylene-*co*-butylene) that was end-capped with hydrogen-bonding ureidopyrimidone groups and CNCs decorated with the same binding motif.[6] Both types of nanocomposites show greatly improved mechanical properties in comparison to the neat supramolecular polymers. A comparison of the two materials systems suggests that dissociation of the reinforcing CNC network during the healing event is important to permit efficient healing. In the former system, this was achieved by limiting the CNC content to 10% w/w. While the mechanical properties of damaged nanocomposites with a higher CNC content could be fully restored, the degree of reinforcement was not as good, presumably on account of some phase separation aided by strong CNC-CNC interactions and weaker CNC-matrix interactions.. In the hydrogen-bonded nanocomposites, where the CNCs were decorated with the same supramolecular motif used to assemble the supramolecular polymer, deliberately introduced defects could be healed quickly and efficiently, even at a filler content of 20% w/w, *i.e.*, in

compositions that exhibit high strength and stiffness. This attractive combination of properties appears to result from the specific design, which leads to full integration of filler and matrix and permits the temporary disengagement of all relevant supramolecular interactions during the healing process.

Thus we report on the preparation and characterization of light-healable nanocomposites based on CNCs and a previously studied (through ARO funding) metallosupramolecular polymer[7] made by the assembly of $Zn(NTf_2)_2$ and a telechelic poly(ethylene-*co*-butylene) that was end-functionalized with 2,6-bis(1′-methylbenzimidazolyl) pyridine (Mebip) ligands (termed BKB). The metal-ligand motifs absorb incident ultraviolet radiation and serve as light-heat converters. Thus, upon irradiation with UV light, the metal-ligand motifs are temporarily dissociated and the material is transformed into a low-viscosity liquid, which can easily fill small defects. When the radiation is switched off, the metallopolymers re-assemble and their original properties are restored. Anticipating that the surface hydroxyl groups of the CNCs can bind to the Zn^{2+} ions and thereby connect the reinforcing filler with the matrix,[8] we sought to explore how the introduction of this filler affects the mechanical properties and healability of these metallopolymers.

Results and Discussion

Preparation of metallosupramolecular nanocomposites

The metallosupramolecular nanocomposites investigated here are based on a previously studied metallosupramolecular polymer7 resulting from the assembly of $Zn(NTf_2)_2$ and a telechelic poly(ethylene-*co*-butylene) end-functionalized with 2,6-bis(1′-methylbenzimidazolyl) pyridine (Mebip) ligands (**Figure 1**). The cellulose nanocrystals used in this work were isolated from microcrystalline cellulose (MCC) according to a previously reported protocol, which affords DMF dispersions of the CNCs.[9] Unless their surface is modified with solubilizing groups, CNCs are usually only well dispersible in polar protic solvents such as water and DMSO,[10] which do not permit dissolution of the metallosupramolecular polymer. However, Dufresne and co-workers[11] recently showed that unmodified CNCs from a sisal source can be temporarily suspended in CH_2Cl_2 via a solvent exchange-process. Adaptation of this protocol permitted for the transfer of the CNCs utilized here from DMF into CH_2Cl_2, which proved to be a suitable solvent for the fabrication of the metallosupramolecular nanocomposites (*vide infra*).

The resulting CNC suspensions were found to be stable for 2 days, before sedimentation of the CNCs was observed. However, it was possible to re-suspend the CNCs in CH_2Cl_2 by a combination of stirring and ultrasonication. TEM images of CNCs that were drop-casted from CH_2Cl_2 (**Figure 2**) confirm that the MCC had indeed been efficiently disintegrated into CNCs and that these CNCs formed homogeneous dispersions in CH_2Cl_2. Analysis of the TEM images revealed that the CNCs transferred into CH_2Cl_2 have an average length of 200 ± 40 nm, a width of 20 ± 2.3 nm, and an aspect ratio of 10. The density of surface charges, presumably stemming from the hydrolysis of the biomass, was determined to be 37 mmol/kg.

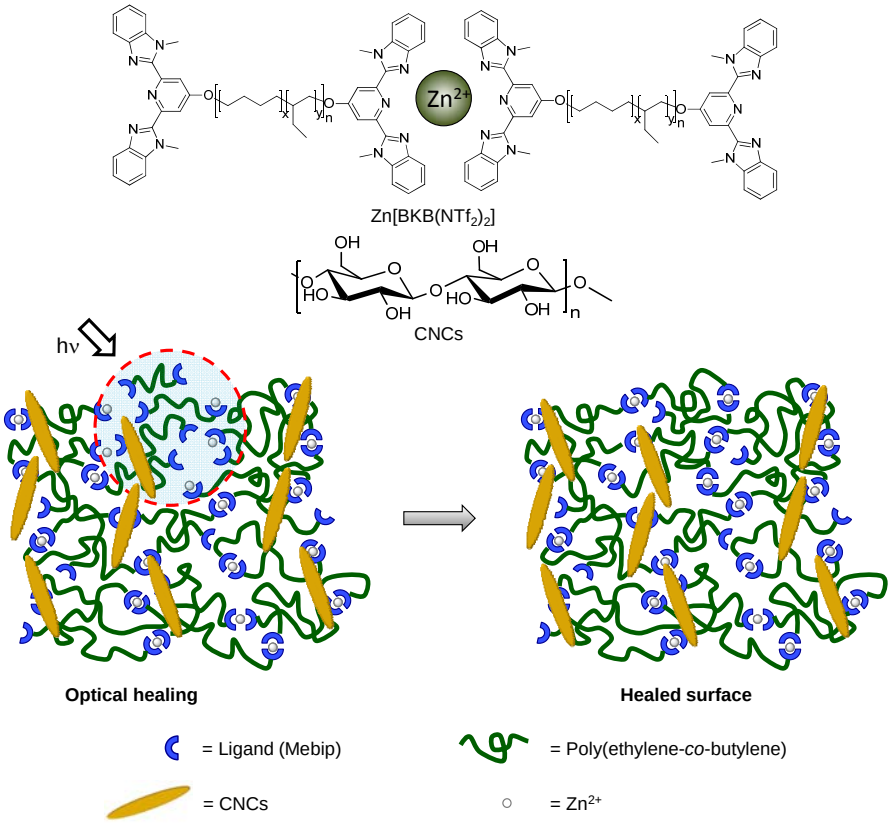

Figure 1. Chemical structure of the metallopolymers $[Zn_xBKB](NTf_2)_2$ and the CNCs, and a schematic representation of the metallosupramolecular nanocomposites.

Figure 2. Transmission electron microscopy (TEM) image of CNCs isolated from microcrystalline cellulose (MCC) and deposited from a suspension in CH_2Cl_2 (0.03 mg/mL) onto a TEM grid and drying the sample at 70 °C for 3 h.

To explore possible interactions between the CNCs and the metallosupramolecular polymer, the BKB macromonomer was titrated with $Zn(NTf_2)_2$ in the presence and absence of CNCs and metal-ligand coordination was monitored by UV-vis spectroscopy. The free Mebip ligand features an absorbance band with a maximum, λ_{max}, at 313 nm (**Figure 3a**). Upon coordination with $Zn(NTf_2)_2$ the absorbance spectrum exhibits a bathochromic shift and the newly formed absorbance of the ligand-to-metal charge transfer (LMCT) transition displays a λ_{max} around 354 nm. Thus, the formation of the metallosupramolecular polymer can be monitored by the decrease of ligand or increase of metal-ligand complex absorbance. Aliquots of $Zn(NTf_2)_2$ were added to a solution of BKB and 10% w/w CNCs (relative to the weight of the BKB) in a 9:1 v/v CH_2Cl_2:CH_3CN solvent mixture; the same experiment was also carried out for the BKB without CNCs. The absorption spectra acquired upon titration of BKB with $Zn(NTf_2)_2$ both in the presence and absence of the CNCs (**Figure 3a**), exhibit an isosbestic point at 327 nm, reflecting a well-defined equilibrium between the free and metal-coordinated ligand.7 Figure 3b shows a normalized absorbance at 354 nm as a function of the Zn^{2+}:BKB ratio for both systems (with and without CNCs), indicative of the formation of the MSP of the sum formula $[Zn_x(BKB)](NTf_2)_2$. In the case of the CNC-free system, the data mirror the previous findings7 and show a discontinuity of the absorbance change at a Zn^{2+}:BKB ratio of 1:1, corresponding to a Zn^{2+}:Mebip ratio of 1:2. In the presence of 10% w/w CNCs, the saturation point is shifted to a

nominal Zn^{2+}:BKB ratio of 1.4:1, indicating that a fraction of the metal ions also bind to the CNCs. This finding is, at least qualitatively, consistent with previous reports that have demonstrated the binding of Zn^{2+} with cellulose, and confirms that the CNCs and the metallosupramolecular polymer, as intended, indeed integrate into supramolecular nanocomposites.

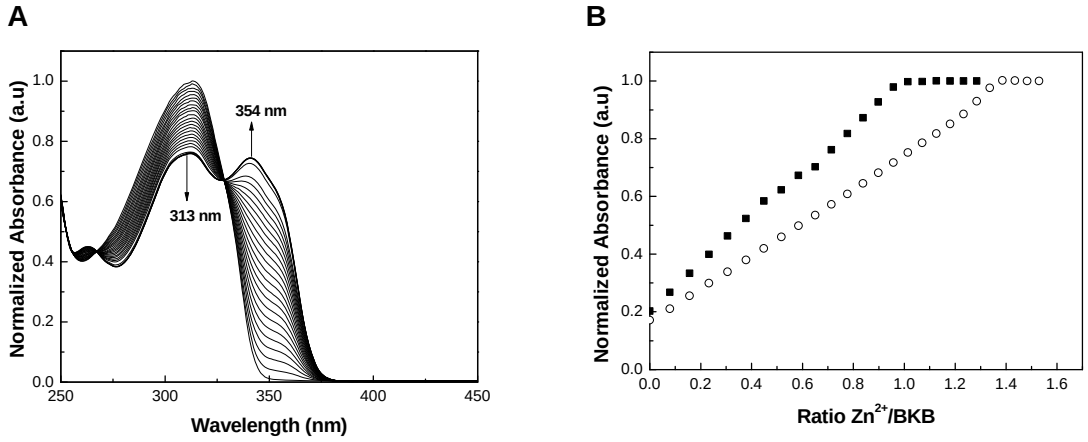

Figure 3. A) UV-vis spectra acquired upon titration of the macromonomer BKB in the presence of CNCs. Data were acquired upon adding aliquots of $Zn(NTf_2)_2$ to a mixture of BKB (25 μM) and CNCs (2 mg/mL, corresponding to 10% w/w with respect to the BKB) in a CH_2Cl_2/CH_3CN (9:1 v/v) solvent mixture. B) Absorption at 354 nm of the spectra recorded as a function of the $Zn(NTf_2)_2$:BKB ratio (○). Also shown are the corresponding data for a titration of the neat BKB without CNCs (■) under otherwise identical conditions.

Reference films of the neat $[Zn_x(BKB)](NTf_2)_2$ (**Figure 4**) were prepared in a similar fashion as recently reported,7 i.e., by combining BKB and $Zn(NTf_2)_2$ in a mixture of CH_2Cl_2 (instead of previously used $CHCl_3$) and CH_3CN (9:1 v/v), evaporation of the solvent, and subsequent compression-molding. Since it was found that in the case of $[Zn_x(BKB)](NTf_2)_2$ a Zn^{2+}:BKB ratio of 1:1 results in the best mechanical properties, but limited healability, whereas a Zn^{2+}:BKB ratio of x = 0.7:1 provides for better healability but lower strength and stiffness (the excess of free ligands renders the system more dynamic), both these compositions were used here as reference materials. The possibility to suspend CNCs in CH_2Cl_2 (*vide supra*) provides a means to readily introduce the cellulose nanofiller into these metallosupramolecular polymers, *i.e.*, by combining CNCs, BKB, and $Zn(NTf_2)_2$ in a mixture of CH_2Cl_2 and CH_3CN. Taking into

consideration the findings of Fox *et al.*,[5] who reported that nanocomposites with high CNC content show a reduced reinforcing effect the CNC content was fixed to 10% w/w relative to the BKB. Nanocomposite films with a varying Zn^{2+}:BKB ratio (x) from 0.7 - 1.5 and a thickness of 350 - 450 μm were prepared by the same process as used here for films of the neat metallosupramolecular polymers. In view of the observation that in the presence of 10% w/w CNCs about a third of the Zn^{2+} ions bind to the cellulose instead of the BKB (**Figure 3b**), and that a third of the Mebip ligands should remain free to promote healing, we expected the nanocomposites with $[Zn_{1.0}(BKB)](NTf_2)_2$ to display the best properties. As can be seen from the pictures shown in Figure 4, films with a Zn^{2+}:BKB ratio x of 0.7 – 1.0 are transparent, suggesting that the CNCs are well dispersed in the metallosupramolecular polymer. At higher Zn^{2+}:BKB ratios (x = 1.2 – 1.4) the materials become opaque, suggesting at least partial aggregation of the CNCs, which is likely due to coordination of the excess of Zn^{2+} to the CNCs. Attempts to create nanocomposites with higher CNC content were made, but they displayed disappointing mechanical properties (*vide infra*).

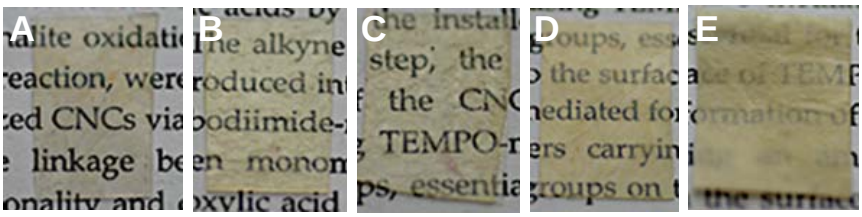

Figure 4. Images of metallosupramolecular nanocomposite films containing 10% w/w CNCs (relative to the BKB) and $[Zn_x(BKB)](NTf_2)_2$ with varying Zn^{2+}:BKB ratio (x). A) CNC/$[Zn_{0.7}BKB](NTf_2)_2$; B) CNC/$[Zn_{0.8}BKB](NTf_2)_2$; C) CNC/$[Zn_{1.0}BKB](NTf_2)_2$; D) CNC/$[Zn_{1.2}BKB](NTf_2)_2$; E) CNC/$[Zn_{1.4}BKB](NTf_2)_2$.

Morphological characterization

Small angle x-ray scattering (SAXS) experiments were performed to determine the influence of the CNCs on the morphology of the metallosupramolecular materials. We note that SAXS and transmission electron microscopy (TEM) studies of films of $[Zn_x(BKB)](NTf_2)_2$ revealed microphase-segregated lamellar morphologies in which the metal-ligand complexes form a hard phase that physically cross-links the soft domains formed by the poly(ethylene-*co*-butylene) segment.[7,12] The SAXS data (**Figure 5**) of the CNC/$[Zn_x(BKB)](NTf_2)_2$ nanocomposites with

varying Zn^{2+}:BKB ratio show distinct correlated Bragg diffraction peaks up to the third order, which confirm that also the nanocomposites with CNC adopt well-ordered layered morphologies. The long period is *ca*. 10 nm, and was determined to be independent of the Zn^{2+}:BKB ratio (x) in these materials. This spatial distance is similar to that observed for the neat $[Zn_xBKB](NTf_2)_2$, for which a spatial distance of *ca*. 8.5 nm was observed.7 We note that the scattering patterns were isotropic, indicating that the domains are not oriented. Interestingly, the lamellar morphology is not perturbed by the presence of CNCs, which have dimensions (diameter = 20 ± 2.3 nm, length = 200 ± 40 nm) that are much larger than the long period of the lamellar morphology. This suggests that the CNCs are not incorporated within the lamellar domains, but reside at the interfaces separating such domains.

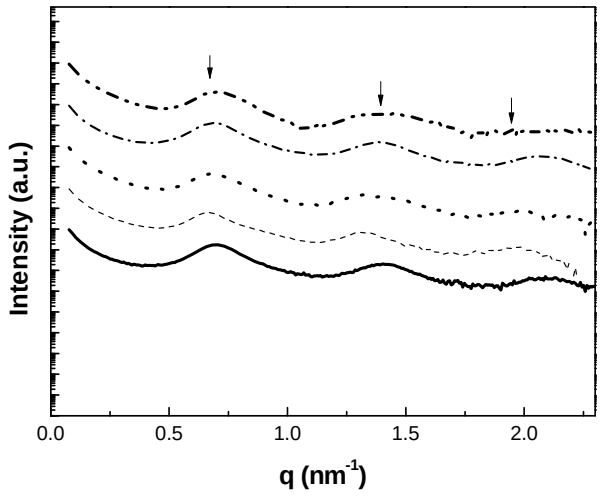

Figure 5. SAXS data for CNC/$[Zn_x(BKB)](NTf_2)_2$ nanocomposites containing 10% w/w CNCs (relative to the BKB) with varying Zn^{2+}:BKB ratio x: (—) CNC/$[Zn_{0.7}BKB](NTf_2)_2$; (---) CNC/$[Zn_{0.8}BKB](NTf_2)_2$; (···) CNC/$[Zn_{1.0}BKB](NTf_2)_2$; (— · —) CNC/$[Zn_{1.2}BKB](NTf_2)_2$; (— · · —) CNC/$[Zn_{1.4}BKB](NTf_2)_2$.

Mechanical Properties

The mechanical properties of thin films of the CNC/$[Zn_x(BKB)](NTf_2)_2$ nanocomposites were explored as a function of temperature by dynamic mechanical thermal analysis (DMTA) (**Figure 6**, **Table 1**) and at room temperature by means of tensile testing (**Figure 7**, **Table 1**). The mechanical properties of neat films of $[Zn_{0.7}(BKB)](NTf_2)_2$ and $[Zn_{1.0}(BKB)](NTf_2)_2$ were

also determined for the purpose of comparison; similar results to previously reported data were obtained for these materials. The DMTA traces of the neat metallosupramolecular polymers, $[Zn_{0.7}(BKB)](NTf_2)_2$ and $[Zn_{1.0}(BKB)](NTf_2)_2$, display a glassy regime below -23 °C, where the tensile storage modulus *E'* is ~2 GPa (**Figure 6**). Above the glass transition a broad rubbery plateau is observed and at 25 °C $[Zn_{0.7}(BKB)](NTf_2)_2$ and $[Zn_{1.0}(BKB)](NTf_2)_2$ display storage moduli of 52 and 60 MPa, respectively. Thus, as previously reported, the stiffness of these materials decrease as the Zn^{2+}:BKB ratio is offset. Stress-strain experiments conducted at 25 °C reveal Young's moduli that mirror this trend and result a maximum stress at break of 1.7 MPa for $[Zn_{0.7}(BKB)](NTf_2)_2$ and 4.7 MPa for $[Zn_{1.0}(BKB)](NTf_2)_2$ (**Figure 7**, **Table 1**).

Gratifyingly, the incorporation of CNCs into the $[Zn_x(BKB)](NTf_2)_2$ matrix led to the desired reinforcement of the metallosupramolecular polymers. Analysis of CNC/$[Zn_x(BKB)](NTf_2)_2$ nanocomposites by DMTA reveals that the materials possess a tensile storage modulus (E') of 2.8-3.1 GPa at -100 °C, which is about 50% higher than in case of the neat $[Zn_x(BKB)](NTf_2)_2$ (**Figure 6, Table 1**). Also in this series, E' is drastically reduced at temperatures above the glass transition. However, the rubbery plateau is shifted to higher moduli in comparison to the two neat reference metallopolymers studied. E' at 25 °C increased steadily with increasing Zn^{2+}:BKB ratio from 77 MPa for CNC/$[Zn_{0.7}(BKB)](NTf_2)_2$ to 135 MPa for CNC/$[Zn_{1.4}(BKB)](NTf_2)_2$. Thus, in comparison to the stiffest matrix polymers ($[Zn_1(BKB)](NTf_2)_2$), E'=60 MPa) the room-temperature modulus of the CNC/$[Zn_x(BKB)](NTf_2)_2$ nanocomposites is increased by a factor of up to 2.5. An inspection of the DMTA traces further shows that the CNCs stabilize the rubbery plateau, i.e., below 100 °C, E' remains relatively constant as a result of stabilization of the CNC network, whereas a steady decrease is observed at increasing temperature in the case of the neat metallopolymers. It should be noted that at higher Zn^{2+} content (greater than the end point of titration with CNCs), a decrease of E' at 25 °C (50 MPa) was observed for a composition of CNC/$[Zn_{1.5}(BKB)](NTf_2)_2$ (**Table 1**). This behavior is likely due to limitations of the degree of polymerization of the MSP, on account of the excess Zn^{2+}. Therefore, a balance between CNC content and Zn^{2+} concentration is necessary to obtain nanocomposite films with improved mechanical properties. Attempts to create nanocomposites with a CNC content of 15 and 20% w/w were made, but the resulting materials Young's moduli and maximum stresses that were lower than those of the materials with only 10% w/w CNCs. This behavior mirrors the observations made by Fox et al.

for nanocomposites based on a supramolecular polymer assembled through π–π interactions with unmodified CNCs,[5] and is consistent with aggregation of the filler.

The DMTA results were complemented with tensile tests (**Figure 7, Table 1**). The Young's modulus changed in a similar manner to *E′* (**Figure 7, Table 1**), the maximum stress increased from 1.7 MPa ($[Zn_{0.7}(BKB)](NTf_2)_2$) to 3.3 MPa (CNC/$[Zn_{0.7}(BKB)](NTf_2)_2$) to 5.6 MPa (CNC/$[Zn_{1.4}(BKB)](NTf_2)_2$), further confirming the reinforcement of $[Zn_x(BKB)](NTf_2)_2$ with CNCs and highlighting the importance of the Zn^{2+}:BKB ratio.

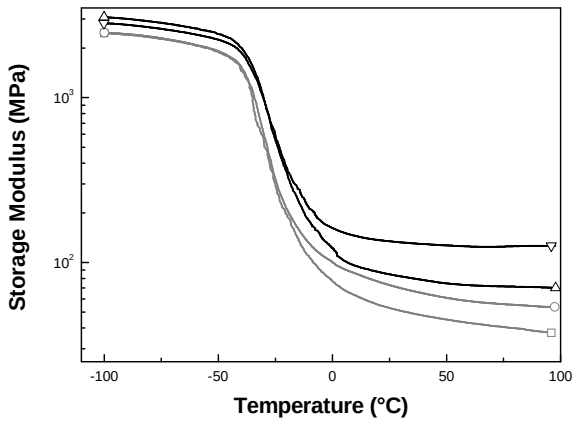

Figure 6. Representative dynamic mechanical thermal analysis (DMTA) traces of the neat metallopolymers $[Zn_{0.7}(BKB)](NTf_2)_2$ (□) and $[Zn_{1.0}(BKB)](NTf_2)_2$ (○) and of the nanocomposites containing 10% w/w CNC and $[Zn_{1.0}BKB](NTf_2)_2$ (8) or $[Zn_{1.4}BKB](NTf_2)_2$ (X). The experiments were conducted at a heating rate of 3°C/min and a frequency of 1 Hz under N_2. Other compositions were also explored.

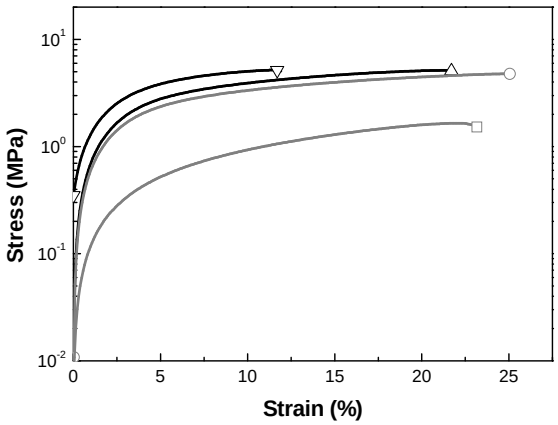

Figure 7. Representative stress-strain curves of the neat metallopolymers $[Zn_{0.7}(BKB)](NTf_2)_2$ (□) and $[Zn_{1.0}(BKB)](NTf_2)_2$ (○) and of CNC/$[Zn_{1.0}BKB](NTf_2)_2$ (8) or CNC/$[Zn_{1.4}BKB](NTf_2)_2$ (X).nanocomposites containing 10% w/w of CNCs. The experiments were conducted at 25°C. Other compositions were also explored.

Table 1. Mechanical properties of $[Zn_xBKB](NTf_2)_2$ and CNC/$[Zn_xBKB](NTf_2)_2$ nanocomposites.

Sample	Storage Modulus[a] (MPa)	Young's Modulus[b] (MPa)	Maximum Stress[b] (MPa)	Strain at Break[b] (%)	Toughness[b] (10^7 J/m^3)
$[Zn_{0.7}BKB](NTf_2)_2$					
original	52 ± 1.0	31 ± 2.2	1.7 ± 0.4	23 ± 5	2.3 ± 0.2
damaged[c]			0.7 ± 0.1	8 ± 1	0.3 ± 0.1
healed[d]		39 ± 5.4	1.5 ± 0.2	30 ± 2	2.9 ± 0.3
$[Zn_{1.0}BKB](NTf_2)_2$					
neat	60 ± 1.4	61 ± 0.7	4.7 ± 0.3	21 ± 1	6.5 ± 0.4
damaged[c]			3.7 ± 0.2	14 ± 1	3.5 ± 1.1
healed[d]		41 ± 1.8	4.0 ± 0.1	15 ± 3	4.1 ± 0.7
CNC/$[Zn_{0.7}BKB](NTf_2)_2$					
original	77 ± 1.1	35 ± 1.6	3.3 ± 0.2	17 ± 2	2.5 ± 0.1

damaged[c]			0.5 ± 0.1	8 ± 2	0.2 ± 0.1
healed[d]		32 ± 2.1	2.8 ± 0.5	14 ± 1	2.3 ± 0.3
CNC/[$Zn_{0.8}$BKB]$(NTf_2)_2$					
original	85 ± 1.4	60 ± 0.5	4.8 ± 0.2	26 ± 2	8.7 ± 0.3
damaged[c]			1.3 ± 0.1	6 ± 2	1.3 ± 1.0
healed[d]		40 ± 6.2	3.4 ± 0.5	23 ± 4	5.7 ± 0.1
CNC/[$Zn_{1.0}$BKB]$(NTf_2)_2$					
Neat	86 ± 6.0	62 ± 10	4.7 ± 0.7	26 ± 1	7.9 ± 0.2
damaged[c]			1.3 ± 0.2	7 ± 3	2.2 ± 0.7
healed[d]		61 ± 8.0	4.6 ± 0.6	24 ± 2	7.7 ± 0.6
CNC/[$Zn_{1.2}$BKB]$(NTf_2)_2$					
original	101 ± 2.0	99 ± 1.3	4.8 ± 1.6	12 ± 3	4.7 ± 0.2
damaged[c]			3.5 ± 0.1	12 ± 1	3.0 ± 0.2
healed[d]		93 ± 4.5	4.8 ± 1.6	14 ± 3	3.6 ± 0.6
CNC/[$Zn_{1.4}$BKB](NTf_2)					
original	135 ± 3.0	101 ± 1.9	5.6 ± 0.2	12 ± 1	4.7 ± 0.2
damaged[c]			3.6 ± 0.1	12 ± 1	3.0 ± 0.2
healed[d]		97 ± 1.4	5.1 ± 0.7	12 ± 3	3.6 ± 0.6
CNC/[$Zn_{1.5}$BKB](NTf_2)					
original	50 ± 3.0	36 ± 3.0	1.0 ± 0.2	9 ± 2	2.7 ± 0.4

[a]Measured by DMTA at 25°C. [b] Measured by stress-strain experiments at 25°C. [c] Samples were damaged in a controlled manner by cutting them to a depth of ~50-70% of their original thickness. [d]Samples were optically healed by exposure to light of a wavelength of 320 to 390 nm and a power density of 950 mW/cm^2 in case of the neat metallopolymers, 350 mW/cm^2 in case of nanocomposites with a Zn^{2+}:BKB ratio x = 0.7 - 1, and 120 mW/cm^2 in the case of nanocomposites with a Zn^{2+}:BKB ratio x = 1.2 - 1.4. Data represent averages from three independently made compositions, from which at least three samples per film were measured.

Optical healing

To explore the healing behavior of CNC/[Zn_x(BKB)]$(NTf_2)_2$ nanocomposites, films of a thickness of 350-400 μm were intentionally damaged by introducing a well-defined cut across the entire sample, with a depth that corresponds to 50-70% of the sample thickness (**Figure 8a,11a**). The samples were subsequently irradiated with UV light of a wavelength range of 320-390 nm, i.e., in the regime where the metal-ligand complexes display a strong absorption band (**Figure 3a**). In the case of the previously studied neat metallopolymers [$Zn_{0.7}$(BKB)]$(NTf_2)_2$ and [$Zn_{1.0}$(BKB)]$(NTf_2)_2$, which were measured for reference purposes, the incident intensity was set to 950 mW/cm^2, corresponding to the conditions employed in the previous study. In the case of the new nanocomposites, the intensity was reduced to 350 mW/cm^2 for nanocomposites with a Zn^{2+}:BKB ratio x of 0.7 - 1, and to 120 mW/cm^2 in the case of nanocomposites with a Zn^{2+}:BKB ratio x = 1.2 - 1.4 eq, as the samples were found to heat excessively at higher intensities; even at the lower intensities used, a rapid temperature increase to >220ºC was observed. Visual inspection confirmed that in all of the materials (**Figures 8, 11**), except for the neat metallopolymer [$Zn_{1.0}$(BKB)]$(NTf_2)_2$, and the CNC/[$Zn_{1.5}$BKB]$(NTf_2)_2$ nanocomposite, the damage imparted to the films could completely or largely be removed by this treatment. . Atomic force microscopy images (**Figure 11**) of a CNC/[$Zn_{0.7}$(BKB)]$(NTf_2)_2$ nanocomposite film containing 10% w/w CNCs film show that the damage zone is indeed filled and the defect completely disappears.

To quantify the healing efficiency of the nanocomposites films, samples of the various compositions were damaged and healed as described above and the mechanical properties of 'original', 'damaged', and 'healed' samples were explored by tensile testing (**Table 1**, **Figure 9**). The healing efficiency was determined by dividing the average toughness of 'original' and 'healed' samples. In Figure 9, representative stress-strain curves of films of the neat metallosupramolecular polymer [Zn_x(BKB)]$(NTf_2)_2$ and the nanocomposite CNC/[$Zn_{1.0}$(BKB)]$(NTf_2)_2$ are shown (the corresponding data for all other compositions are shown in **Table 1**). The data show that in all compositions, the stress and strain at break of damaged samples are significantly reduced in comparison to the original materials. Conversely, the original mechanical properties of the materials are largely restored upon UV irradiation (**Table 1, Figure 10**). Statistical experiments (**Table 1, Figure 10**). reveal that the toughness of healed samples are slightly lower than the toughness of original, nonetheless, the original

mechanical properties are nearly fully recovered. These results are in agreement with recently published work from our group based on supramolecular nanocomposites composed of a hydrogen-bonded supramolecular polymer and cellulose nanocrystals.

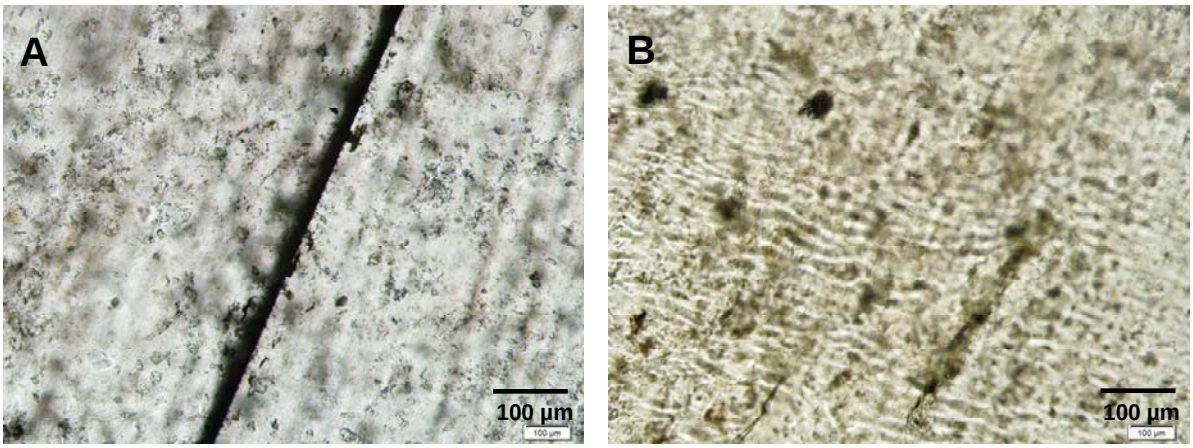

Figure 8. Optical microscopy images of a deliberately damaged CNC/[Zn_x(BKB)]$(NTf_2)_2$ nanocomposite film containing 10% w/w CNCs (A) before and (B) after healing through exposure to UV light (320-390 nm, 30 s, 350 mW/cm^2).

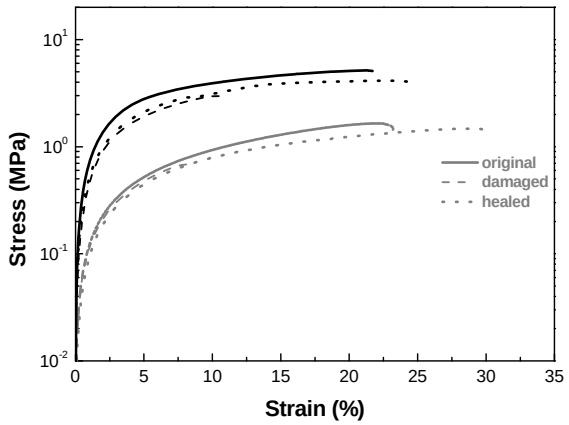

Figure 9. Representative stress-strain curves of films of the neat metallopolymer [$Zn_{0.7}$(BKB)]$(NTf_2)_2$ (grey) and of the CNC/[$Zn_{1.0}$BKB]$(NTf_2)_2$ nanocomposites comprising 10% w/w CNC (black). Shown are data acquired at 25° C for original (—), damaged (- - -), and healed (···) samples. Samples were damaged by applying a cut of a depth of 50-70% of the thickness and healed through a 30 s exposure to light of a wavelength of 320-390 nm and an intensity of 950 mWcm^{-2} in case of the neat metallopolymer and 350 mWcm^{-2} in case of the nanocomposite.

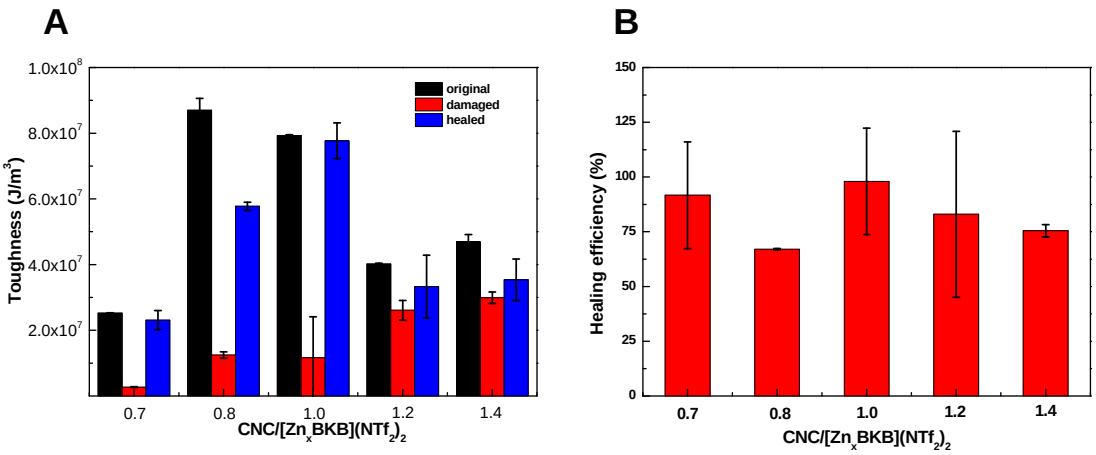

Figure 10. A) Toughness of original, damaged, and healed CNC/[Zn_x(BKB)]$(NTf_2)_2$ nanocomposite films containing 10% w/w CNCs. The toughness was calculated from the area under the stress-strain curves and represents an average for n = 3 - 5 measurements; error bars express standard deviation. B) Healing efficiency of the metallosupramolecular nanocomposite films (n = 3-5 ± standard deviation). Samples were damaged in a controlled manner by cutting them to a depth of ~50-70% of their original thickness and optically healed by exposure to light of a wavelength of 320 to 390 nm and a power density of 950 mW/cm^2 in case of the neat metallopolymers, 350 mW/cm^2 in case of nanocomposites with a Zn^{2+}:BKB ratio x = 0.7-1, and 120 mW/cm^2 in the case of nanocomposites with a Zn^{2+}:BKB ratio x = 1.2-1.4.

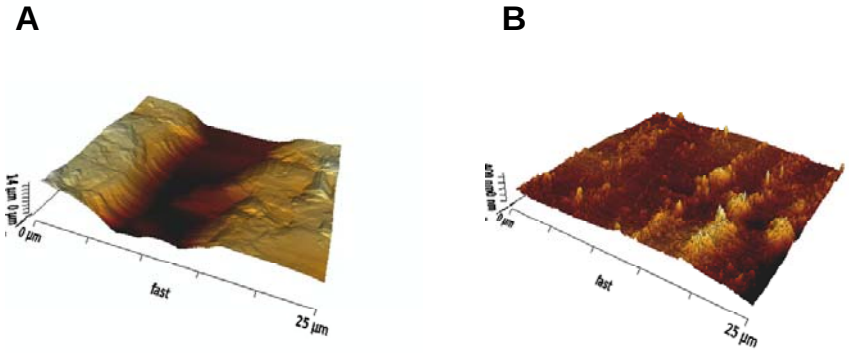

Figure 11. AFM images of a damaged CNC/[$Zn_{0.7}$(BKB)]$(NTf_2)_2$ nanocomposite film containing 10% w/w CNCs (A) before and (B) after healing with UV light (320-390 nm, 30 s, 350 mW/cm^2).

In conclusion, this work demonstrates that metallosupramolecular materials can be reinforced with cellulose nanocrystals to improve the mechanical strength while also allowing for optical healing behavior. These properties suggest that a balance between the coordination of metal salt by the cellulose nanocrystals and ligand-functionalized polymer render the system dynamic. In combination with the optical properties of the Zn^{2+}-Mebip complexes, a sufficient light-heat conversion initiates the depolymerization of the metallosupramolecular polymer, thus allowing for efficient healing of these materials. Due to the tunable nature of the polymer backbone, ligands, and metal ions, this framework can be adapted to other types of chromophores, binding motifs, and stimuli.

1.2. Toward Photo-labile metallosupramolecular healable polymers

Our previously reported metallosupramolecular healable polymers, which employ Zn(II) or Eu(III) complexes, utilize a direct photo/thermal process that requires relatively large temperatures (150-200 °C) to be reached in order to induce healing, which necessitates the use of high light intensities (320-390 nm, 30 s, 900 mW/cm^2).[7] The use of such intense light and high temperatures dramatically limits the type of polymer that can be healed without exhibiting significant degradation. In fact to date we have only reported the photohealing of polymers based on a telechelic poly(ethylene-*co*-butylene) end-functionalized with 2,6-bis(1′-methylbenzimidazolyl) pyridine (Mebip) ligands (termed BKB). Furthermore, it can be difficult to use the photo/thermal process to achieve these high healing temperatures if the polymer is on thermally-conducting substrates (e.g., glass or metal) that act as heat-sinks. Thus in an attempt to extend the utilization of metal-ligand polymer complexes for rapid photohealing applications to other polymer structures and expand the use of these metallosupramolecular polymers to access healable coatings for thermally conducting substrates, we sought to explore different a metal/ligand complex where the metal ligand complex could be significantly weekend upon exposure to light.

There are several reports in the literature that describe the photodissociation of Fe(II) metal-ligand complexes at or below room temperature.[13,14,15] In polypyridine complexes it has been proposed that this relates to a photo-induced spin crossover in the Fe(II) complex converting it from a low spin ground state to an high spin excited state. The length of the Fe(II)-ligand bond

has been shown to increase in this excited state suggesting a weakening of the complex resulting in more labile ligands[16],[17] and photodissociation.[16] Consequently, we hypothesized that if Fe(II) was used as the coordinating metal in the metallo-supramolecular polymer films, then it would be possible to access healable materials that would require greatly reduced light intensities opening the door to a wider range of polymeric materials that could be photo-healed on a broader range of substrates including ones, such as glass, that act as heat sinks.

To explore the photo-healing of Fe(II) metal-ligand complexes in polymeric materials, we prepared ditopic 2,6-bis(1′-methylbenzimidazolyl)pyridine (Mebip) end-capped poly(tetrahydrofuran) polymer (BTB) films at a 1:1 (Fe(II):BKB) ratio. We first wanted to determine if these systems could heal on a nonthermally-conducting substrate and used electrical tape as previously described for Zn(II):BKB metallosupramolecular polymers. The Fe(II):BTB films were intentionally cut all the way through one side of the film with a razor blade (**Figure 12**; bottom). The films were then placed on electrical tape and irradiated with an unfiltered UV-vis light source for 2 x 30 seconds. The films successfully mended at a light intensity of 460 mW/cm^2, which is a much lower intensity than was reported for the similar Zn(II):BKB systems which healed at 900 mW/cm^2.7

As a control, we similarly prepared Zn(II):BTB polymeric networks at a 0.7:1. This metal:ligand ratio was reported as the optimal ratio for the healing of the Zn(II):BKB films. Upon light irradiation on similarly damaged films (**Figure 12**; top row), the Zn(II) polymeric films burned at a light intensity of 460 mW/cm^2. We repeated the tests at lower light intensities, but consistently yielded unhealed films. This result was unsurprising since it was previously reported that Zn(II) complexes require higher intensities of UV exposure for the photo/thermal dissociation of the metal/ligand complex to occur (*vide supra*).[7]

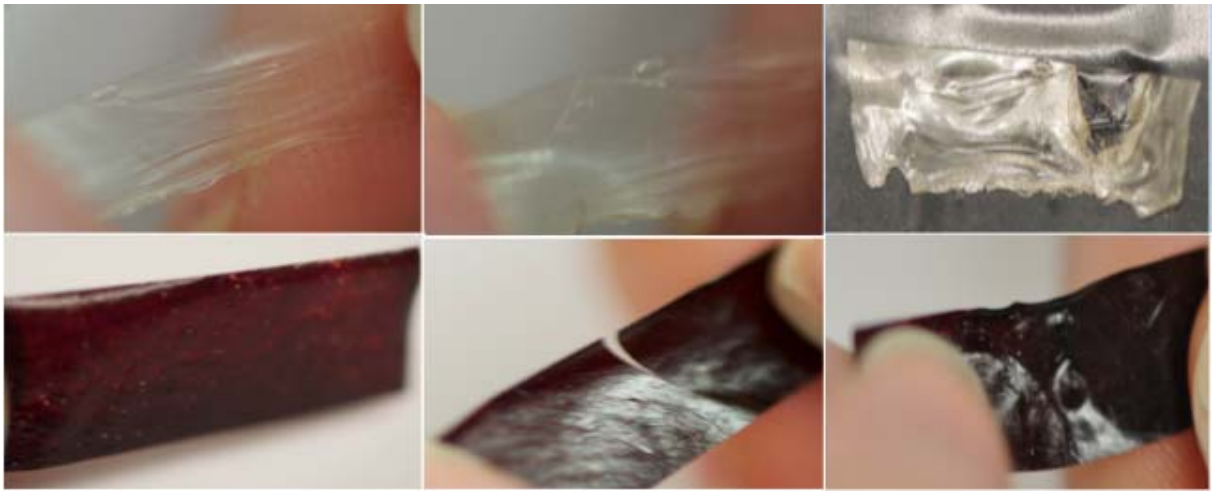

Figure 12. ***Top row***: Wavelength – entire spectrum. Film dimensions: Width – 4.97 mm; thickness – 70 μm; (left) Neat Zn(II):BTB 0.7:1 film; (middle) Damaged Zn(II):BTB 0.7:1 film; (right) Zn(II):BTB 0.7:1 film after 2 x 30s UV exposure. Light intensity – 460 mW/cm^2. ***Bottom row***: Light intensity – 436 mW/cm^2. Film dimensions: Width – 7.69 mm; thickness – 700 μm; (left) Neat Fe(II):BTB 1:1 film; (middle) Damaged Fe(II):BTB 1:1 film; (right) Fe(II):BTB 1:1 film after 2 x 30s UV exposure.

Since the ultimate goal was to determine if Fe(II) metallosupramolecular polymers could heal on a thermally conducting substrate, we again prepared a Fe(II):BTB (at a 1:1 ratio) polymeric films. The film was cut through on one side (**Figure 13** – bottom), but this time placed on a metal block as the substrate for healing experiments. The damaged film was irradiated with an unfiltered UV-vis light source at an intensity of 436 mW/cm^2. Since the film was cut all the way through, the two flaps near the damaged area were overlapped to ensure that each side was touching. Remarkably, the two flaps of the film successfully mended together after 2 x 30s UV exposure. As a control, we similarly tested the healing of Zn(II):BTB (at a 0.7:1 ratio) polymeric films on the metal block (**Figure 13** – top). These films burned after 3 x 30s UV exposure at a light intensity of 462 mW/cm^2. Furthermore, we repeated these tests of the Zn(II) polymeric films at lower light intensities, but consistently resulted in unhealed films. These preliminary results not only demonstrate that the Fe(II) complexes allow for direct photohealing of damaged polymer films at lower light intensities than previously reported systems, but also expands on the range of photo-healable coated both in the chemical structure of the metallosupramolecular polymer as well as the substrates they can be coated on. Mechanical testing of the healed

samples is underway to compare the material properties of the neat versus healed films. Finally, we will test the application of these systems as photorelease adhesives between thermally conducting substrates.

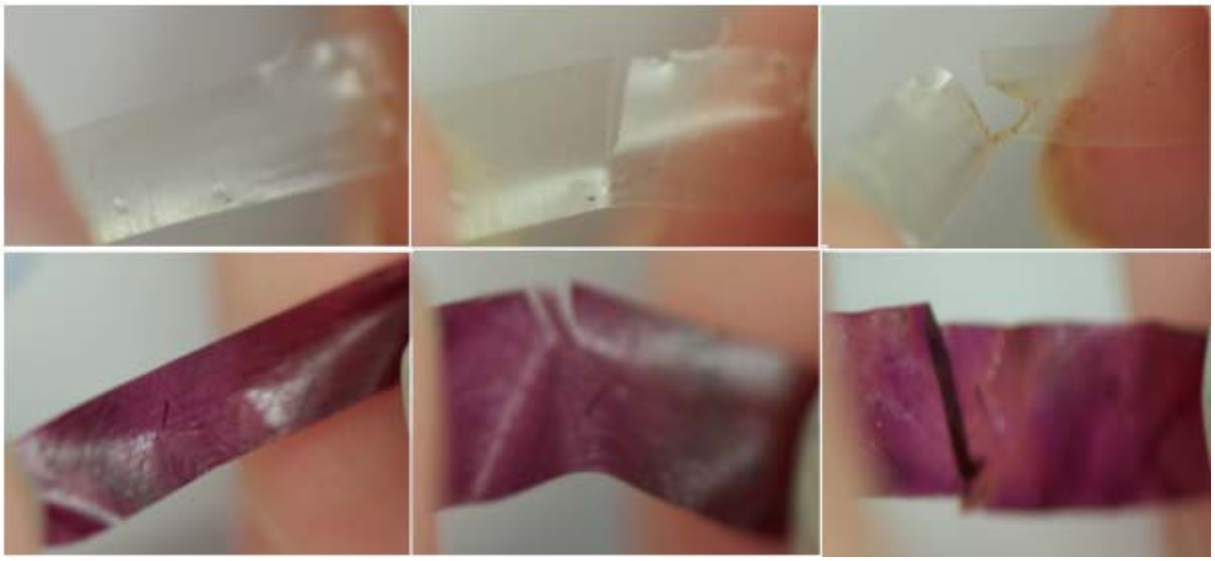

Figure 13. ***Top row***: Light intensity – 462 mW/cm^2. Wavelength – entire spectrum. Film dimensions: Width – 4.01 mm; thickness – 60 μm; (left) Neat Zn(II):BTB 0.7:1 film; (middle) Damaged Zn(II):BTB 0.7:1 film; (right) Zn(II):BTB 0.7:1 film after 3 x 30s UV exposure. ***Bottom row***: Light intensity – 436 mW/cm^2. Film dimensions: Width – 5.13 mm; thickness – 10 μm: (left) Neat Fe(II):BTB 1:1 film; (middle) Damaged Fe(II):BTB 1:1 film; (right) Fe(II):BTB 1:1 film after 2 x 30s UV exposure.

References

1 Bergman, S. D.; Wudl, F. *J. Mater. Chem.* **2008**, *18*, 41.

2 Fiore, G. L.; Rowan, S. J.; Weder, C. *Chem. Soc. Rev.* **2013**, *42*, 7278.

3 (a) Camarero Espinosa, S.; Kuhnt, T.; Foster, E. J.; Weder, C. *Biomacromolecules* **2013**, *14*, 1223. (b) Changsarn, S.; Mendez, J. D.; Shanmuganathan, K.; Foster, E. J.; Weder, C.; Supaphol, P. *Macromol. Rapid Commun.* **2011**, *32*, 1367. (c) Dagnon, K. L.; Shanmuganathan, K.; Weder, C.; Rowan, S. J. *Macromolecules* **2012**, *45*, 4707. (d) Kumar, S.; Hofmann, M.; Steinmann, B.; Foster, E. J.; Weder, C. *ACS Appl. Mater. Interfaces* **2012**, *4*, 5399. (e) Mendez, J.; Annamalai, P. K.; Eichhorn, S. J.; Rusli, R.; Rowan, S. J.; Foster, E. J.; Weder, C.

Macromolecules **2011**, *44*, 6827. (f) Way, A. E.; Hsu, L.; Shanmuganathan, K.; Weder, C.; Rowan, S. J. *ACS Macro Lett.* **2012**, *1*, 1001.
4 (a) Eichhorn, S. J.; Dufresne, A.; Aranguren, M.; Marcovich, N. E.; Capadona, J. R.; Rowan, S. J.; Weder, C.; Thielemans, W.; Roman, M.; Renneckar, S.; Gindl, W.; Veigel, S.; Keckes, J.; Yano, H.; Abe, K.; Nogi, M.; Nakagaito, A. N.; Mangalam, A.; Simonsen, J.; Benight, A. S.; Bismarck, A.; Berglund, L. A.; Peijs, T. *J. Mater. Sci.* **2010**, *45*, 1. (b) Habibi, Y.; Lucia, L. A.; Rojas, O. J. *Chem. Rev.* **2010**, *110*, 3479. (c) Klemm, D.; Kramer, F.; Moritz, S.; Lindström, T.; Ankerfors, M.; Gray, D.; Dorris, A. *Angew. Chem., Int. Ed.* **2011**, *50*, 5438. (d) Eichhorn, S. J. *ACS Macro Lett.* **2012**, *1*, 1237.
5 Fox, J.; Wie, J. J.; Greenland, B. W.; Burattini, S.; Hayes, W.; Colquhoun, H. M.; Mackay, M. E.; Rowan, S. J. *J. Am. Chem. Soc.* **2012**, *134*, 5362.
6 Biyani, M. V.; Foster, E. J.; Weder, C. *ACS Macro Lett.* **2013**, *2*, 236.
7 Burnworth, M.; Tang, L.; Kumpfer, J. R.; Duncan, A. J.; Beyer, F. L.; Fiore, G. L.; Rowan, S. J.; Weder, C. *Nature* **2011**, *472*, 334.
8 (a) Richards, N. J.; Williams, D. G. *Carbohydr. Res.* **1970**, *12*, 409. (b) Xu, Q.; Chen, L.-F. *J. App. Polym. Sci.* **1999**, *71*, 1441.
9 Capadona, J. R.; Shanmuganathan, K.; Trittschuh, S.; Seidel, S.; Rowan, S. J.; Weder, C. *Biomacromolecules* **2009**, *10*, 712.
10 van den Berg, O.; Capadona, J. R.; Weder, C. *Biomacromolecules* **2007**, *8*, 1353.
11 Siqueira, G.; Bras, J.; Dufresne, A. *Biomacromolecules* **2009**, *10*, 425.
12 Kumpfer, J. R.; Wie, J. J.; Swanson, J. P.; Beyer, F. L.; Mackay, M. E.; Rowan, S. J. *Macromolecules* **2011**, *45*, 473.
13 Child, C. R.; Kealey, S.; Jones, H.; Miller, P. W.; White, A. J. P.; Gee, A. D.; Long, N. J. *Dalton Trans.* **2011**, *40*, 6210-6215.
14 Simon, A.; Joblin, C. *J. Phys. Chem. A* **2009**, *113*, 487.
15 Hauser, A. *Chem. Phys. Lett.* **1990**, *173*, 507.
16 Gallé, G.; Jonusauskas, G.; Tondusson, M.; Mauriac, C.; Letard, J. F.; Freysz, E. *Chem. Phys. Lett.* **2013**, *556*, 82.
17 Holyer, R. H.; Hubbard, C. D.; Kettle, S. F. A.; Wilkins, R. G. *Inorg. Chem.* **1966**, *5*, 622.